Appendix

Table of content

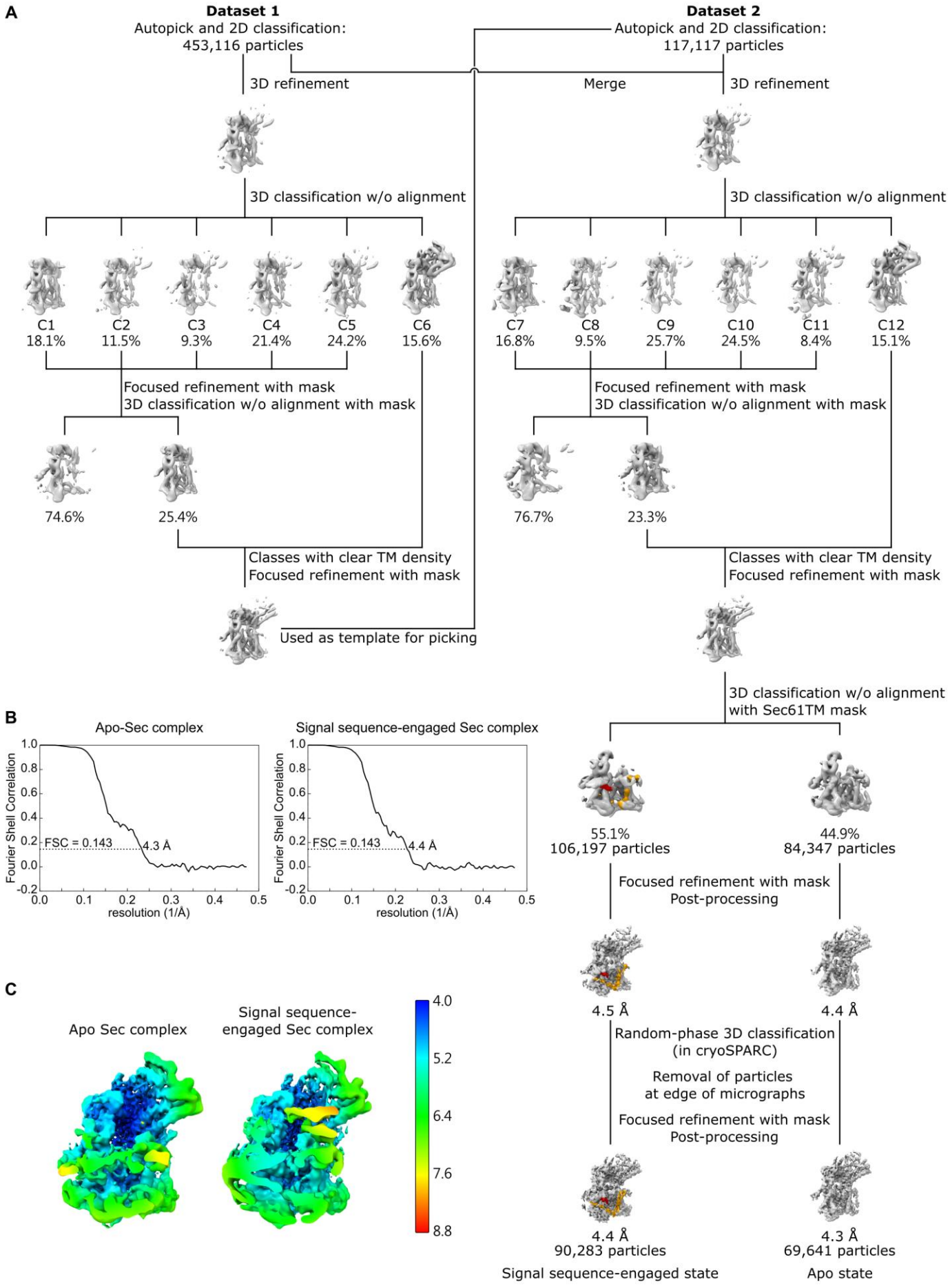

Appendix Figure S1. Cryo-EM single particle analysis of the signal sequence-bound Sec complex

A. 3D classification scheme. A total of 453,116 particles from dataset 1 was selected after 2D classification and refined. The following 3D classification into six classes showed one class with clear density for the TM region. The other five classes were joined and further 3D classified with a soft binary mask focusing on the TM region. All classes with clear TM density were joined and refined using the same mask. This refined map was used as a template for particle picking on dataset 2. A total of 117,117 particles from dataset 2 was selected after 2D classification. The two datasets were then merged and the same 3D classifications were performed again to obtain a map with clear TM density. A third 3D classification was performed only focusing on the Sec61 complex. This revealed one class with extra density for the Sec62 TM helices and the other class lacking this extra density. These two classes were again focused refined resulting in the 4.5 Å and 4.4 Å resolution structures of the signal sequence-bound and apo heptameric complex, respectively. Random-phase 3D classification was performed to further remove bad particles, and particles at the edge of micrographs were also removed. This resulted in the final 4.4 Å and 4.3 Å reconstructions of the signal-sequence bound and apo Sec complex, respectively.

B. Gold standard Fourier Shell Correlation (FSC) resolution curves of the final 3D reconstructions of the ss-bound and apo Sec complex.

C. 3D reconstructions of the ss-bound and apo Sec complexes low-pass filtered and color-coded according to local resolution. For clarity, density for the detergent micelle was masked.

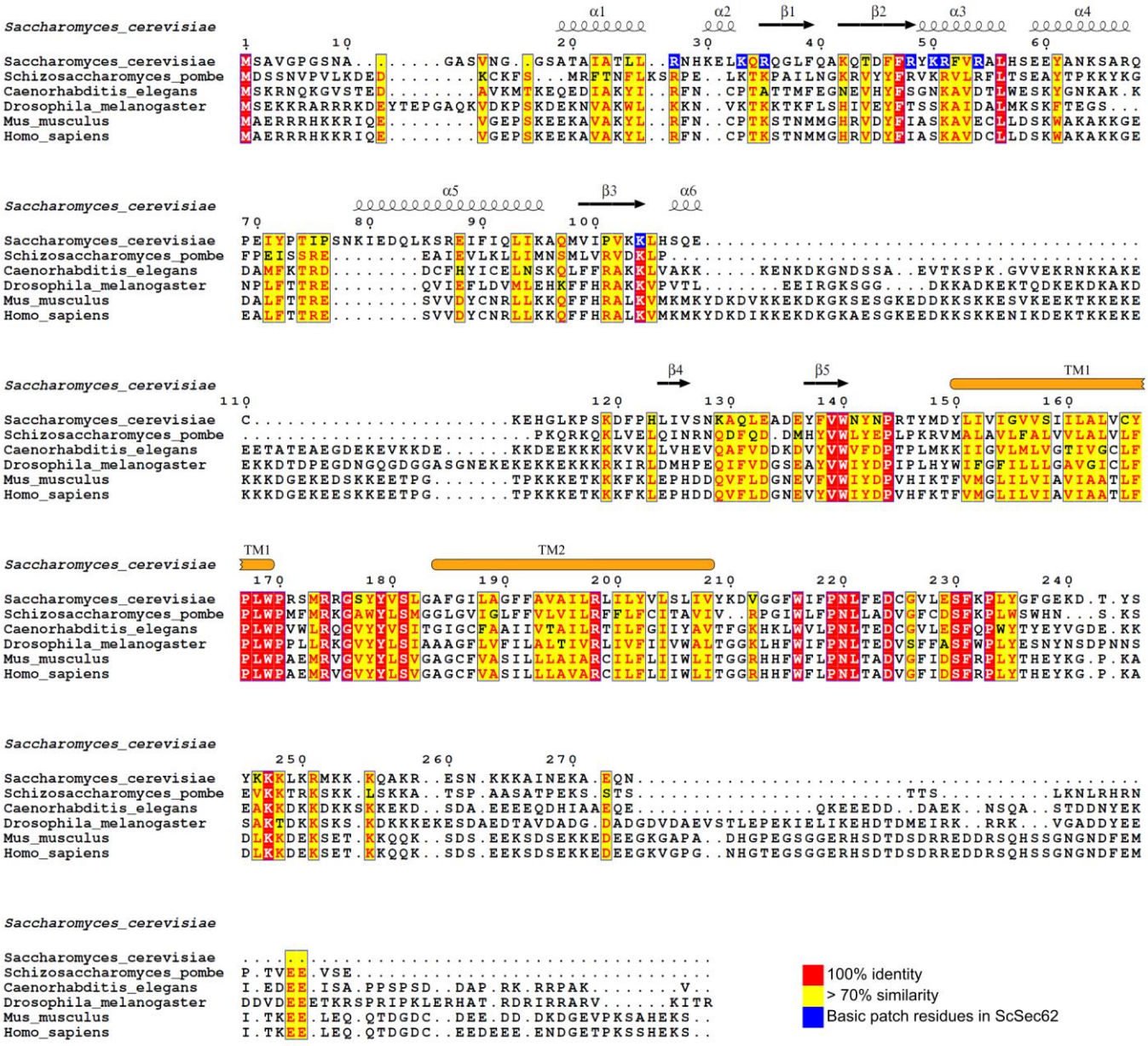

Appendix Figure S2. Multiple protein sequence alignment of Sec62

The multiple sequence alignment was performed with T-Coffee program (Notredame *et al*, 2000) and was plotted using ESPript (http://espript.ibcp.fr) (Robert & Gouet, 2014). The secondary structure of the Sec62 domain and the predicted TMs (orange bars) are shown above the sequences.

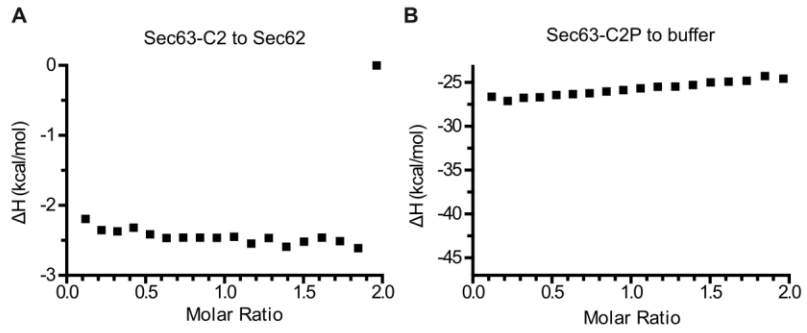

Appendix Figure S3. Isothermal titration calorimetry analysis of Sec63-C2 with Sec62 domain

A. ITC thermogram from the titration of the Sec62 domain with the Sec63-C2 peptide.

B. ITC thermogram from the buffer control.

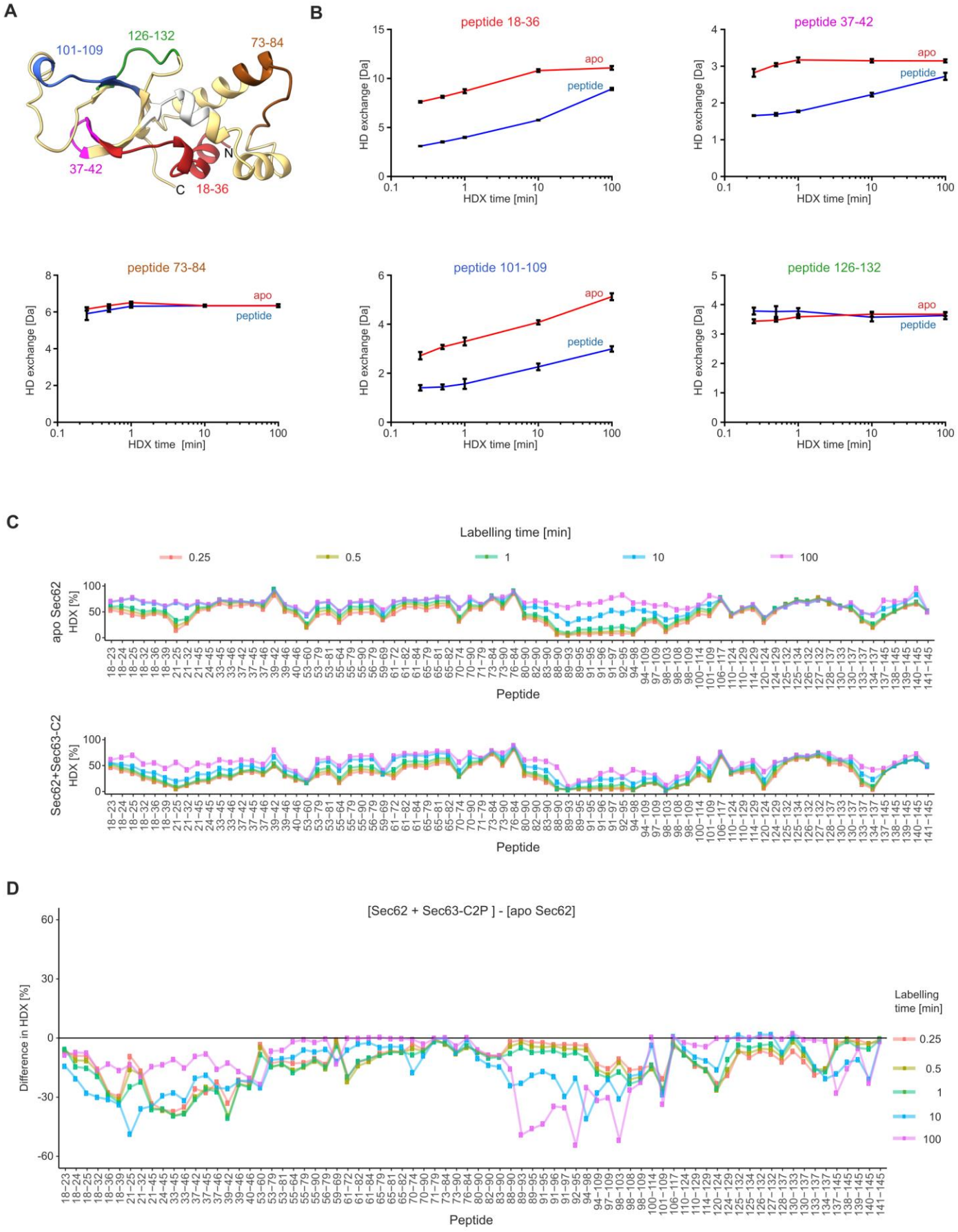

Appendix Figure S4. Mapping the binding site of the Sec63 C-terminus to the Sec62 domain by HDX MS

A. After the HDX experiment, the Sec62 domain was digested and the peptides were analyzed by MS. The location of analyzed peptides was marked in the crystal structure of Sec62 domain.

B. Hydrogen-deuterium exchange (HDX) plot of five representative peptides derived from the Sec62 domain. Data represent the mean ± SD (n = 3 technical replicates).

C. Relative HDX of all peptides identified for Sec62 in absence or presence of the Sec63-C2P peptide.

D. Difference in relative HDX between the Sec62 domain/Sec63-C2P complex and Sec62 domain only.

Appendix References

Notredame C, Higgins DG & Heringa J (2000) T-Coffee: A novel method for fast and accurate multiple sequence alignment. *J Mol Biol* 302: 205–217

Robert X & Gouet P (2014) Deciphering key features in protein structures with the new ENDscript server. *Nucleic Acids Res* 42: W320–W324